Enhanced Core Polarization in ^{70}Ni and ^{74}Zn

O. Perru,[1] O. Sorlin,[1,9] S. Franchoo,[1] F. Azaiez,[1] E. Bouchez,[2] C. Bourgeois,[1] A. Chatillon,[2] J. M. Daugas,[3] Z. Dlouhy,[4] Zs. Dombrádi,[5] C. Donzaud,[1] L. Gaudefroy,[1] H. Grawe,[6] S. Grévy,[7] D. Guillemaud-Mueller,[1] F. Hammache,[1] F. Ibrahim,[1] Y. Le Coz,[2] S. M. Lukyanov,[8] I. Matea,[9,*] J. Mrazek,[4] F. Nowacki,[10] Yu.-E. Penionzhkevich,[8] F. de Oliveira Santos,[9] F. Pougheon,[1] M. G. Saint-Laurent,[9] G. Sletten,[11] M. Stanoiu,[1] C. Stodel,[9] Ch. Theisen,[2] and D. Verney[1]

[1]*Institut de Physique Nucléaire, IN2P3-CNRS, F-91406 Orsay Cedex, France*
[2]*CEA-Saclay, DAPNIA-SPhN, F-91191 Gif sur Yvette Cedex, France*
[3]*CEA/DIF/DPTA/SPN, B.P. 12, F-91680 Bruyères le Châtel, France*
[4]*Nuclear Physics Institute, AS CR, CZ 25068, Rez, Czech Republic*
[5]*Institute of Nuclear Research, Postfach 51, H-4001 Debrecen, Hungary*
[6]*GSI, Postfach 110552, D-64200 Darmstadt, Germany*
[7]*LPC, ISMRA, F-14050 Caen Cedex, France*
[8]*FLNR, JINR, 141980 Dubna, Moscow region, Russia*
[9]*GANIL, B.P. 5027, F-14076 Caen Cedex, France*
[10]*IReS, IN2P3-CNRS, Université Louis Pasteur, B.P. 28, F-67037 Strasbourg Cedex, France*
[11]*NBI, University of Copenhagen, Copenhagen, Denmark*

(Received 17 May 2005; revised manuscript received 26 April 2006; published 13 June 2006)

The reduced transition probabilities $B(E2; 0^+ \rightarrow 2_1^+)$ of the neutron-rich ^{74}Zn and ^{70}Ni nuclei have been measured by Coulomb excitation in a ^{208}Pb target at intermediate energy. These nuclei have been produced at Grand Accélérateur National d'Ions Lourds via interactions of a 60A MeV ^{76}Ge beam with a Be target. The $B(E2)$ value for $^{70}\mathrm{Ni}_{42}$ is unexpectedly large, which indicates that neutrons added above $N = 40$ strongly polarize the $Z = 28$ proton core. In the Zn isotopic chain, the steep rise of $B(E2)$ values beyond $N = 40$ continues up to $^{74}\mathrm{Zn}_{44}$. The enhanced proton core polarization in ^{70}Ni is attributed to the monopole interaction between the neutron in the $g_{9/2}$ and protons in the $f_{7/2}$ and $f_{5/2}$ spin-orbit partner orbitals. This interaction could result in a weakening of magicity in $^{78}\mathrm{Ni}_{50}$.

DOI: 10.1103/PhysRevLett.96.232501 PACS numbers: 25.70.De, 21.30.Fe, 23.20.Js, 27.50.+e

Shell structure predictions towards the neutron drip line provide indispensable input to model the rapid neutron-capture nucleosynthesis [1]. Furthermore, the evolution of shell structure far off the stability line has become a key topic of nuclear structure studies, as it is intimately related to the monopole part of the residual nucleon-nucleon interaction and its origin in one-boson exchange potentials [2]. The evolution of single particle energies and shell gaps has been recently ascribed to the strongly attractive (repulsive) tensor force acting between protons and neutrons with opposite (similar) orientation of their intrinsic spin with respect to their angular momentum [3]. Along an isotopic chain of proton-magic nuclei, the reduced transition probability $B(E2; 0^+ \rightarrow 2^+)$ value provides a sensitive signature of shell evolution. Within a generalized seniority scheme [4,5] which exploits the property of nucleons paired to $J = 0^+$ in nearby orbitals, the $B(E2; 0^+ \rightarrow 2^+)$ values follow a parabola (see, for instance, Ref. [6]) proportional to $f(1 - f)$, where f is the fractional filling of the neutron shell. For a nucleus with N neutrons located between two adjacent closed shell isotopes with neutron numbers N_1 and N_2, it is expressed as $f = (N - N_1)/(N_2 - N_1)$. As neutrons are chargeless particles, the height of the parabola depends on the strength of neutron-induced proton core excitations. Any deviation from the parabolic curve indicates structural changes: (i) a reduction indicating a (sub)shell closure, (ii) an increase pointing to deformation through strong proton-neutron interaction, and (iii) a constantly small $B(E2)$ hints for a decoupling of protons and neutrons.

Recently, the Ni isotopes between the $N = 28$ and 50 shell closures have been the subject of extensive experimental and theoretical studies [7–14]. For $28 \leq N \leq 40$, a parabolalike trend was found [11] in the $B(E2; 0^+ \rightarrow 2^+)$ values which seemed to indicate a subshell closure at $N = 40$. On the other hand, the two-neutron separation energies exhibit a smooth decrease at $N = 40$ [9,15] rather than a sharp drop. High-spin states in ^{68}Ni and ^{70}Ni can be described in a simple shell-model approach taking pure neutron configurations into account [8,9,16], while the 2 proton holes neighbor nucleus ^{66}Fe exhibits a rather collective behavior already at low excitation energy [17]. Beyond $N = 40$, a striking reduction in the 2^+ excitation energies is observed from ^{70}Ni to ^{76}Ni [18] which could be due to increasing collectivity. A direct measurement of the $B(E2; 0^+ \rightarrow 2^+)$ value in the Ni and Zn isotopes should evidence this effect.

We report here the results of the first measurements of the $B(E2; 0^+ \rightarrow 2^+)$ of $^{74}_{30}\mathrm{Zn}_{44}$ and $^{70}_{28}\mathrm{Ni}_{42}$. These nuclei were produced at the Grand Accélérateur National d'Ions Lourds (GANIL) facility via reactions of a 60A MeV $^{76}\mathrm{Ge}^{30+}$ beam with an average intensity of 1.2 $e\mu$A in a 500 μm-thick Be target. Two settings of the LISE3 spectrometer [19] were used to select these isotopes. Mean

rates of 4200 and 800 per second were obtained for the ^{74}Zn and ^{70}Ni isotopes, respectively. Another spectrometer setting was set to transmit the $q = 28^+$ charge state of the primary beam at a rate of 10^4 s^{-1} in the same optical conditions. This aimed to confirm the known $B(E2)$ value of ^{76}Ge [20], which has subsequently been used as a reference to determine the $B(E2)$ values of ^{74}Zn and ^{70}Ni. Nuclei were identified by means of their energy loss and time of flight measured in a ''removable'' Si detector placed downstream from the spectrometer at the entrance of the target chamber. This detector was inserted several times during each spectrometer setting to determine the ratio of nuclei of interest over the total number of transmitted nuclei.

Coulomb excitation at $v/c \sim 0.28$ for ^{74}Zn and ^{70}Ni and 0.29 for ^{76}Ge was induced in a ^{208}Pb target of 120 mg/cm^2 thickness located at the focal plane of LISE3. The target was surrounded by four segmented clover Ge detectors of the EXOGAM gamma array placed at 90° at a distance of 5.5 cm from the target, yielding a total photopeak efficiency of $\epsilon_\gamma = 5.0\%$ at 1.3 MeV.

Two x-y drift chambers were mounted at 27 and 47 cm downstream from the ^{208}Pb target in order to reconstruct the trajectories of the emergent nuclei after their interaction. This allows one to determine the diameter of the beam spot at the target location. Within the error bars, a FWHM of 11.4(6) mm was found for all nuclei, which ensures that all Coulomb excitations were measured under the same geometrical conditions.

Two annular Si detectors, with internal (external) diameters of 3 cm (9 cm), were mounted 56 cm behind the target in order to identify the deflected nuclei by their energy losses and residual energies. In the case of ^{76}Ge, the angular coverage ranged from 1.5° to 6.1° in the center of mass frame, the grazing angle being 6.2°. By using the calculated angular distribution of the nuclei after Coulomb deflection from Ref. [21] distorted by the angular straggling of the nuclei into the target, a Monte Carlo simulation shows that about 25% of the nuclei that underwent Coulomb excitation either flew through the central hole of the annular Si detector or were deflected at larger angular values. The ratios ϵ_{geom} of Coulomb excited nuclei that were detected in the annular Si detector to the total number of deflected nuclei are listed in Table I for the three nuclei ^{76}Ge, ^{74}Zn, and ^{70}Ni. Nuclei emerging with smaller angles were detected in a plastic scintillator 2 m downstream which served to determine the total number of implanted nuclei. The number N_n of nuclei of interest impinging on the target are given in Table I. It was derived from the yields obtained in the removable Si detector and in the plastic scintillator, the latter triggering the acquisition system at a reduced calibrated rate of 2%. The ratio of ^{74}Zn over the total number of transmitted nuclei was 68(2)% over the 18 hours of accumulated beam time. That for ^{70}Ni was 10.2(9)% along the 3 days of beam time accumulated for this nucleus. In this latter spectrometer setting, 7.7(7)% of ^{74}Zn were also transmitted. The proportion of the 8^+ isomer in the ^{70}Ni beam was measured to be 1.4(2)%. Any contribution of the isomer decay to the yield of $2^+ \rightarrow 0^+$ γ rays attributed to the Coulomb excitation process is negligible.

TABLE I. Experimental parameters used to deduce $B(E2)_{\text{rel}}$ values relative to that of ^{76}Ge: N_n is the number of nuclei impinging on the target, N_γ the number of γ rays due to Coulomb excitation. ϵ_{geom} and ϵ_{ang} are the geometrical and angular correction factors (see text).

Isotope	N_n (10^8)	N_γ	ϵ_{geom}	ϵ_{ang}	$B(E2)_{\text{rel}}$ (e^2 fm^4)
^{76}Ge	2.19(2)	6450(150)	0.78	1.06	2680(80)[a]
^{74}Zn	2.78(8)	5630(140)	0.74	1.06	2040(150)
^{70}Ni	1.58(14)	675(90)	0.75	0.98	860(140)

[a]Ref. [20].

Photons emitted in flight in coincidence with the scattered nuclei were detected in the four segmented EXOGAM Ge clover detectors. The segmentation of the clover detectors allowed us to reduce the Doppler broadening by 40%, leading to an energy resolution (FWHM) of 75 keV at 1 MeV. The Doppler-corrected spectra for the ^{76}Ge, ^{74}Zn, and ^{70}Ni nuclei are shown in Fig. 1. They exhibit photopeaks associated with the Coulomb excitation of the 2^+ energy level. The structure of the γ background is very similar for all nuclei, as shown in the right part of Fig. 1. The number of γ rays in the peaks N_γ is given in Table I.

During the Coulomb excitation process, a certain amount of angular momentum alignment is present while ejectiles are emitted at very forward angles. As compared to an isotropic γ-ray distribution, the $\Delta\ell = 2$ γ rays emitted in flight exhibit two lobes focused at the forward direction according to the Lorentz energy boost. However, the rate of γ rays, within the laboratory angular coverage of 78°–120°, was close to that of an isotropic source as the loss of photons at backward angles was compensated by the gain of photons at forward angles. The angular efficiency relative to that of a calibration source located at the ^{208}Pb target position ϵ_{ang} is listed in Table I.

Applying the correction factors ϵ_{geom} and ϵ_{ang} to the experimental cross section, we find a Coulomb excitation cross section up to the grazing angle of $\sigma(0^+ \rightarrow 2^+) = 1070(100)$ mb for ^{76}Ge. The EXCAMP code [22] determines, for a given $B(E2)$ value, the integrated semiclassical Coulomb excitation cross section [21]. The present $\sigma(0^+ \rightarrow 2^+)$ for ^{76}Ge corresponds to $B(E2) = 2990(270)e^2$ fm^4, in agreement with the value of $2680(80)e^2$ fm^4 [20] derived from low-energy Coulomb excitation studies. To minimize systematical effects in the determination of the absolute $B(E2)$ values, the $B(E2)$

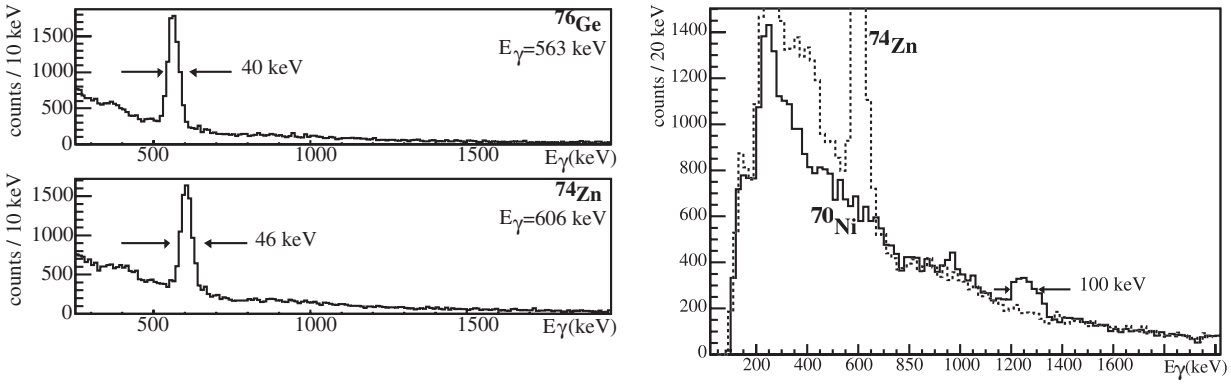

FIG. 1. Doppler-corrected γ-energy spectra obtained in the Ge clover detectors from the Coulomb excitation of the ^{76}Ge, ^{74}Zn, and ^{70}Ni isotopes. Spectra of ^{74}Zn (dashed line) and ^{70}Ni (solid line) are superimposed in the right part, showing clearly the 1260 keV peak attributed to the $0^+ \rightarrow 2^+$ excitation of ^{70}Ni.

values of ^{70}Ni and ^{74}Zn in Table I have been determined relative to that of ^{76}Ge [20]. For ^{74}Zn, we have additionally found a consistent $B(E2)$ value of $1970(240)e^e$ fm^4 from the $1.25(12) \times 10^8$ ^{74}Zn which were transmitted in the spectrometer setting dedicated to the study of ^{70}Ni. The agreement between the $B(E2)$ value of ^{76}Ge determined by low- and high-energy Coulomb excitation adds evidence that contributions to the measured $2^+ \rightarrow 0^+$ γ transition from a nuclear process or/and from the side feeding by higher lying excited states are minor. This is confirmed for the three studied nuclei by the fact that one does not observe any other γ line in their spectra which would arise from the deexcitation of high-lying states, as, in particular, from the known 2_2^+ states in ^{76}Ge [20], ^{74}Zn [23], and ^{70}Ni [12].

The behavior of the $B(E2; 0^+ \rightarrow 2^+)$ values (Fig. 2) is used in the following to gauge the role of the $N = 40$ subshell closure and the evolution of collectivity in the Ni and Zn isotopic chains. In the Ni isotopic chain, the $\pi f_{7/2}$ orbital is separated from the remaining proton orbitals of the fp shell by the $Z = 28$ gap. In the Zn isotopic chain, valence protons in the $\pi p_{3/2}$ and $\pi f_{5/2}$ orbitals (above the $Z = 28$ gap) also add to polarization by proton-neutron interaction besides their direct contribution to the $E2$ strength. Below $N = 40$, the $B(E2)$ curve reaches a maximum in the Ni and Zn chains at or near midoccupation by neutrons of the fp shell ($N = 34$) and subsequently decreases until $N = 38$. The parabolic curve in the proton-magic Ni chain follows the trend of a generalized seniority scheme for a $\Delta v = 2$ transition [4–6,24]. As the neutron fp orbitals are progressively filled, the core polarization occurs through quadrupole excitations via $\pi f_{7/2}^{-1} p_{3/2}$ configurations [7,11]. The offset of the parabola below $N = 40$ in the Zn isotopic chain is caused by the two added valence protons. The large scale shell model reproduces the Ni and Zn $B(E2)$ curves below midshell $N = 34$ within a fp model space [25,26], while for $N \geq 34$ the $g_{9/2}$ neutron orbit is essential for a correct description as shown in Refs. [11,26].

At $N = 40$, the $B(E2; 0^+ \rightarrow 2^+)$ value reaches a minimum in the Ni chain. Such a minimum has been ascribed mainly to the lack of $E2$ excitation between the fp and the $g_{9/2}$ orbitals of different parity value [9,11,13]. In the Zn isotopic chain, the minimum is shifted to $N = 38$, which does not necessarily document an $N = 38$ subshell closure as suggested in Ref. [24]. From the calculated occupancies of the $\nu g_{9/2}$ orbital (n) shown in Fig. 2, it is seen that the pairing correlations ([11,13]) start to empty the fp orbitals in the Zn isotopic chain earlier and to a larger extent than in Ni (i.e., $n = 1.2$ for ^{68}Ni and 2.9 for ^{70}Zn). The enhanced filling of the $\nu g_{9/2}$ orbit at $N = 40$ in the Zn chain brings a direct contribution to the $B(E2; 0^+ \rightarrow 2^+)$ value through the $(\nu g_{9/2})^2$ configuration, in contrast to the Ni isotopic chain. This displaces the $B(E2)$ minimum from $N = 40$ in the Ni isotopes to $N = 38$ in the Zn isotopic chain.

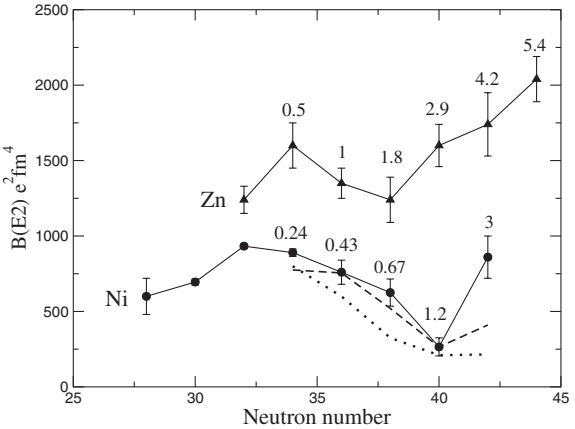

FIG. 2. Experimental $B(E2; 0^+ \rightarrow 2^+)$ values in units of e^2 fm^4 in the Ni and Zn isotopic chains. Results on ^{70}Ni and ^{74}Zn nuclei are from the present study. Other values are taken from Refs. [20,34]. The number of neutrons in the $g_{9/2}$ orbital [written on top of each $B(E2)$ curve] and the $B(E2)$ values in Ni are calculated with the shell model of Ref. [11] (dashed line) or with the QRPA model of Ref. [13] (dotted line).

Beyond $N = 40$, the present work indicates a steep rise for ^{70}Ni, even within the experimental uncertainties. In the Zn isotopes, the $B(E2)$ values continue to increase with N with the expected parabolic trend at least towards the $g_{9/2}$ midshell ($N \simeq 44$). We can infer the amount of the ^{68}Ni core polarization of the 2^+ state in ^{70}Ni through the evolution of the $B(E2; J \rightarrow J-2)$ values along the 8^+, 6^+, 4^+, 2^+ components of the $(\nu g_{9/2})^2$ multiplet. We expect the 8^+ state of this multiplet to be almost only of neutron origin, as a 8^+ spin value cannot be built with protons in the fp orbitals. The $B(E2; 8^+ \rightarrow 6^+)$ would therefore correspond to a reference value for the weakest core polarization. Recently, $E2$ transition strengths were determined [27–29] for high-spin states in ^{70}Ni, and a new empirical $T = 1$ effective interaction was derived in the pure neutron $p, f_{5/2}, g_{9/2}$ model space [30]. In this approach, the experimental $B(E2; 8^+ \rightarrow 6^+) = 19(4)$ [27], $B(E2; 6^+ \rightarrow 4^+) = 43(1)$ [28,29], and the present $B(E2; 2^+ \rightarrow 0^+) = 172(28) e^2\,\mathrm{fm}^4$ are calculated as 17.3, 44.6, and $92.2 e^2$ fm^4, respectively, using an effective neutron charge $e\nu = 1.2e$. The good agreement for the high-spin states breaks down for the $2^+ \rightarrow 0^+$ transition, which is a clear signature for an enhanced proton core polarization at low excitation energy. This conclusion is at variance with the quasi-random-phase approximation (QRPA) [13] and shell-model results [11] (see Fig. 2) which predict that the low-energy $B(E2)$ strength in ^{70}Ni predominantly corresponds to neutron excitations, decoupled from the proton core.

The strong polarization in the Ni and Zn isotopes beyond $N = 40$ could be due to the attractive $\pi f_{5/2}$-$\nu g_{9/2}$ monopole interaction [31–33], ascribed to the tensor force of the in-medium nucleon-nucleon interaction [3]. This force is also predicted to act through the repulsive $\pi f_{7/2}$-$\nu g_{9/2}$ interaction to reduce the apparent $\pi f_{7/2}$-$\pi f_{5/2}$ spin-orbit splitting. From these mutual interactions, the effective $Z = 28$ shell gap and the $N = 40$ subshell gap are reduced as neutrons are added in the $g_{9/2}$ orbital, favoring the development of collectivity. This hypothesis is supported by the fact that the experimental $B(E2)$ values in the Zn isotopic chain scale with the calculated occupation of the $\nu g_{9/2}$ orbital (cf. Fig. 2).

In summary, the $B(E2; 0^+ \rightarrow 2^+)$ values of ^{70}Ni and ^{74}Zn have been determined for the first time. The $B(E2)$ value of $^{70}\mathrm{Ni}_{42}$ increases by a factor of 3, as compared to $^{68}\mathrm{Ni}_{40}$, indicating that the filling of the neutron $g_{9/2}$ shell induces a rapid polarization of the proton core. The $B(E2)$ value is still increasing with the neutron number at ^{74}Zn, which corresponds to midoccupancy of the neutron $g_{9/2}$ orbital. The strong polarization effect beyond $N = 40$ has been ascribed to the $\pi f_{5/2}$-$\nu g_{9/2}$ neutron-proton interaction which plays an essential role for rapidly bringing collectivity above $Z = 28$ as neutrons are added in the $g_{9/2}$ shell. It is foreseen that this hitherto poorly studied part of the nucleon-nucleon force would influence the behavior of shell closures far from stability as, in particular, the effectiveness of the magicity of ^{78}Ni.

We thank the EXOGAM Collaboration for providing the segmented-clover detectors. This work was partially supported by the following funding agencies: EU TMR ERBSMGECT 950036, OTKA Contract No. T46901, GA AS Czech Rep. No. A1048 605, INTAS 00-00463. We thank J. Kiener for providing us useful advices and the EXCAMP code.

*Present address: CENBG, B.P. 120, le Haut Vigneau, F-33175 Gradignan Cedex, France.

[1] B. Pfeiffer *et al.*, Nucl. Phys. **A693**, 282 (2001).
[2] T. Otsuka *et al.*, Phys. Rev. Lett. **87**, 082502 (2001).
[3] T. Otsuka *et al.*, Phys. Rev. Lett. **95**, 232502 (2005).
[4] I. Talmi, in *Elementary Modes of Excitation in Nuclei*, Proceedings of the International School of Physics "Enrico Fermi," edited by A. Bohr and R. A. Broglia (North-Holland, Amsterdam, 1977), p. 352.
[5] R. F. Casten, in *Nuclear Structure from a Simple Perspective*, edited by P. E. Hodgson (Oxford University Press, New York, 1990), p. 121.
[6] A. Holt *et al.*, Nucl. Phys. **A634**, 41 (1998).
[7] O. Kenn *et al.*, Phys. Rev. C **63**, 064306 (2001).
[8] T. Ishii *et al.*, Phys. Rev. Lett. **84**, 39 (2000).
[9] H. Grawe *et al.*, in *Tours Symposium on Nuclear Physics IV: Tours 2000*, edited by M. Arnould *et al.*, AIP Conf. Proc. No. 561 (AIP, New York, 2001), p. 287.
[10] A. M. Oros-Peusquens and P. F. Mantica, Nucl. Phys. **A669**, 81 (2000).
[11] O. Sorlin *et al.*, Phys. Rev. Lett. **88**, 092501 (2002).
[12] M. Sawicka *et al.*, Phys. Rev. C **68**, 044304 (2003).
[13] K. H. Langanke *et al.*, Phys. Rev. C **67**, 044314 (2003).
[14] P. T. Hosmer *et al.*, Phys. Rev. Lett. **94**, 112501 (2005).
[15] C. Guénaut *et al.*, Eur. Phys. J. A **25**, 33 (2005).
[16] R. Grzywacz *et al.*, Phys. Rev. Lett. **81**, 766 (1998).
[17] M. Hannawald *et al.*, Phys. Rev. Lett. **82**, 1391 (1999).
[18] C. Mazzochi *et al.*, Phys. Lett. B **622**, 45 (2005).
[19] R. Anne and A. C. Mueller, Nucl. Instrum. Methods Phys. Res., Sect. B **70**, 276 (1992).
[20] S. Raman *et al.*, At. Data Nucl. Data Tables **78**, 1 (2001).
[21] A. N. F. Aleixo and C. A. Bertulani, Nucl. Phys. **A505**, 448 (1989).
[22] J. Kiener (private communication).
[23] J. A. Winger *et al.*, Phys. Rev. C **39**, 1976 (1989).
[24] I. Deloncle and B. Roussière, nucl-th/0309050.
[25] O. Kenn *et al.*, Phys. Rev. C **63**, 021302(R) (2001).
[26] O. Kenn *et al.*, Phys. Rev. C **65**, 034308 (2002).
[27] M. Lewitowicz *et al.*, Nucl. Phys. **654**, 687c (1999).
[28] H. Mach *et al.*, Nucl. Phys. **A719**, C213 (2003).
[29] M. Stanoiu, Ph.D. thesis, Caen (GANIL Report No. T03-01, 2003).
[30] A. Lisetskiy *et al.*, Phys. Rev. C **70**, 044314 (2004).
[31] S. Franchoo *et al.*, Phys. Rev. Lett. **81**, 3100 (1998).
[32] H. Grawe, in *The Euroschool Lectures on Physics with Exotic Beams, Vol. I*, Lecture Notes in Physics Vol. 651 (Springer, Berlin-Heidelberg, 2004), p. 33.
[33] N. Smirnova *et al.*, Phys. Rev. C **69**, 044306 (2004).
[34] S. Leenhardt *et al.*, Eur. Phys. J. A **14**, 1 (2002).